Title

Spectroscopic investigation of wheat grains (Triticum aestivum) infected by wheat seed gall nematodes (Anguina tritici)

Authors

Singh, Vivek Kumar
Devi, Anjana
Pathania, Surbhi
et al.

Publication Date

2017

DOI

10.1016/j.bcab.2016.11.005

Peer reviewed

Analysis of plant leaves using Laser Ablation-Inductively Coupled Plasma Optical Emission Spectrometry: Use of Carbon to compensate for matrix effects

[1,2]José Chirinos, [2]Dayana Oropeza, [2,3]Jhanis González*, Vassilia Zorba[2] and [2,3]Richard E. Russo

[1]Escuela de Química, Facultad de Ciencias, Universidad Central de Venezuela, Caracas 1041a, Venezuela.

[2]Lawrence Berkeley National Laboratory, Berkeley, CA, USA.

[3]Applied Spectra, Inc., Fremont, CA, USA.

---

* Author to whom correspondence should be addressed

Telephone: + 1 510 4952899

Fax: +1 510 483 7303

E-mail: jjgonzalez@lbl.gov

ABSTRACT

Direct solid sampling by Laser Ablation into an Inductively Coupled Plasma Synchronous Vertical Dual View Optical Emission Spectroscope (LA-SVDV-ICP OES) was used for the elemental analysis of nutrient elements Ca, B, Mn, Mg, K and Zn and essential (non-metallic) elements P and S in plant materials. The samples were mixed with paraffin as a binder, an approach that provides better cohesion of the particles in the pellets in addition to supplying carbon to serve as an internal standard (atomic line C I 193.027 nm) as a way to compensate for matrix effects, and/or variations in the ablation process. Precision ranged from 1 to 8 % relative standard deviation (RSD) with limit of detection ranging from 0.4 to 1 and 25 to 640 mg kg^{-1} for metallic and non-metallic elements, respectively.

Keywords: laser ablation, inductively coupled plasma optical emission spectrometry, plant samples.

INTRODUCTION

The essential nutrient elements in plants can be classified into two groups: macronutrients at percentage concentrations such as N, P, K, Mg, Ca, S, and micronutrients, at mg kg^{-1} levels such as Fe, Mn, Zn, Cu, Ni, B, Mo, and Cl. The determination of these elements is important as changes in concentration could compromise essential functions in plant metabolism. For example, deficiency of N, P and S could affect the protein synthesis and energy transport in plants[1]. Other examples where essential elements play key roles are: i) Mg in the photosynthesis process, ii) K, Fe, Mn, Zn, Cu, Mo and Ni in the activation of enzymes, and iii) Ca and B in cell wall synthesis and/or stabilization.[1, 2]

Atomic Absorption Spectroscopy (AAS), Inductively Coupled Plasma Optical Emission Spectroscopy (ICP-OES) and Inductively Coupled Plasma Mass Spectrometry (ICP-MS) play a vital role in the elemental analysis of plants samples. Typically, solid plant materials are digested with strong acids and/or high temperature ashing procedures[3-9]. Even though the implementation of solid sample digestion is common and in many cases routine, the process is time-consuming, increases the risk of contamination, and generates chemical waste. Quantitative analysis protocols that reduce the complexity of sample preparation are therefore critical for environmental and ecological applications.

Solid in liquids dispersions or slurries,[10] as well as direct electrothermal vaporization[11] and laser ablation[12-13] have been used in both ICP-OES and ICP-MS to avoid the tedious wet digestions methods. These solid sampling techniques have practical benefits such as minimum sample pretreatment, small risk of contamination and reduced chemical waste generation, all leading to rapid multielement analysis directly from the solid.

Laser ablation for direct solid sampling is a compelling approach for rapid chemical analysis. Sampling involves a high-power pulsed laser beam that is directed and focused onto a sample to instantaneously convert a finite volume of the sample into vapor and aerosol constituents for analysis. Laser ablation of solid samples is commonly used in combination with two detection modalities: Laser Induced Breakdown Spectroscopy (LIBS) and Laser Ablation-Inductively Coupled Plasma-Mass Spectrometry (LA-ICP-MS) or Laser Ablation- Inductively Coupled Plasma Optical Emission Spectrometry (LA-ICP-OES).[14-16] Successful applications have been recently demonstrated in metallomic studies of plant materials using laser ablation-based techniques, namely LIBS and LA-ICP- MS or LA-ICP-OES.[17-25] A brief description of these techniques will help understand the selection of LA-ICP-OES for the analysis of plant materials as the focal point of this study. LIBS offer direct and in-situ analysis of potentially the entire periodic table of elements. It is important to further emphasize that LIBS could be use to analyze elements likes hydrogen, oxygen, nitrogen, fluorine and halogens that are difficult or impossible to analyze by other techniques. LIBS also posses some key features such as low cost of operation (no gas requirements), portability, stand-off detection, etc. However limits of detection (which are in the high ppm range for most elements) still one of the major limitations of this technique. In contrast LA-ICP-MS main attributes are high sensitivity (in the low ppm to ppb level for most elements) plus isotopic information. However, quantification of some of the essential elements in plants using low resolution ICP-MS is challenging due to interferences in the mass range between 30-80 amu, for example interferences of $^{38}Ar^{1}H$ on ^{39}K, ^{40}Ar on ^{40}Ca, and $^{40}Ar^{16}O$ on ^{56}Fe are particularly critical. In the particular case of these interferences the use of higher resolution ICP-MS or ICPMS equipped with collision/reaction cell technology is recommended, however it is also important to highlight that in those cases sensitivity will be

sacrifice in order to reduce/eliminate or resolve these interferences.

Laser Ablation Inductively Coupled Plasma Optical Emission Spectroscopy (LA-ICP-OES) is an attractive approach and capitalizes on ICP-OES as one of the most commonly found and widely used instruments in analytical laboratories. The main reason for this is the ICP-OES robustness, ease of use, and relatively low operational cost. Remarkably LA-ICP-OES is not as widely used for quantitative analyses of plant materials compared to LIBS and LA-ICP-MS, even though LA-ICP-OES offers simultaneous multi-element detection capability, with low limit of detection (in the single digit ppm range for most elements) and, in general, high spectral selectivity by using high-resolution spectrometers to avoid or minimize spectral interferences. In particular modern ICP-OES instruments with dual view technology offer an increased dynamic range of concentration (from low ppm level to major (%) elements present in samples) by combining the capability of collecting emission for elements emitting in the UV spectral region axially, and elements emitting in the visible region radially from the same ablation event.[25]

The primarily goal of this study was to explore the benefits of the synchronous vertical dual view mode (SVDV) ICP-OES for determination of essential elements in plants using laser ablation as a sampling tool. In this study were also addressed two different matrix effects: a "natural matrix effect" which is related to the natural differences between the samples, and a "synthetic matrix effect" which is generated when a binder is added to the samples.

EXPERIMENTAL

Instrument

The ablation system was the J200 from Applied Spectra, Inc. using a Nd:YAG nanosecond laser at 213 nm wavelength. The ablation chamber could accommodate samples up to 100 mm diameter with flexibility in volume and washout time. This system was interfaced to the 5100 SVDV-ICP-OES (Agilent, Santa Clara, CA, USA). **Table 1** shows a list of the optimized conditions used in all these experiments. Laser ablation was performed with helium as the carrier gas. Argon was used as a make-up gas before entering the ICP-OES plasma and to purge the spectrometer.

Reagents and samples

Four plant certified reference materials (powder form with 75 μm particle size) were used in this work; apple leaves (SRM 1515), peach leaves (SRM 1547), spinach leaves (SRM 1570a) and tomato leaves (1573a) from the National Institute of Standard and Technology (NIST, Gaithersburg, MD, USA) (**Table** 2). Study of natural matrix effect is based on the comparison among pure samples, and study of the synthetic matrix effect was based on a suite of samples prepared by mixing the pure standards with different amounts (mass fractions) of paraffin binder having particle size lower than 30 μm (3646 Spex, Metuchen, NJ, USA). Adding paraffin to the pure samples not only dilutes the elemental concentration but it also becomes the matrix after a sufficiently amount (concentration) has been added to the mixture.

Each of the four SRM samples was mixed with paraffin at proportions from 10% to 90% in 10% increments. The mass fractions of the standard in the pellets were from 0-100 %, with 0% meaning pure paraffin and 100% pure standard. The samples were weighed and mixed for five minutes to ensure homogenization. Following homogenization, the powders including pure paraffin were pelletized (Spex model 3630) with about 7 tons of pressure. Paraffin only contains

hydrogen and carbon (C_nH_{2n+2}). This was verified by analysis of the pure paraffin pellet under the same experimental conditions and none of the elements of interest in the plants were detected**.**

Methods

Ablation sampling method

The samples were ablated with a laser repetition rate of 10 Hz while moving the sample at a speed 0.025 $mm.s^{-1}$. Using the Agilent ICP-OES software ICP-Expert®, signals were acquired in the time resolved analysis mode (TRA). The transient signals were integrated using the Applied Spectra, Inc. Data Analysis software. Analytical figures of merit such as limit of detection, precision within one location (temporal relative standard deviation (TRSD)), and the precision between ablation locations (relative standard deviation (RSD)) of three raster lines on the samples were determined. The standard deviation of the background was obtained from the pure paraffin pellet (labeled as 0% mass fraction of the standard). The LODs were calculated as 3.3 s/b, where s is the standard deviation of the signal obtained from the blank pellet, and b is the slope of the calibration curve.[26] The apple standard that has the lowest concentration of the analytes was used in this study.

Use of Carbon to compensate matrix effects

Matrix effects can lead to poor accuracy during quantification analysis in most analytical techniques, and in particular for laser ablation-based quantitative analysis; these effects are triggered in general by different ablation behavior between samples and standards used for quantification.[27-29] Differences in ablation behavior are manifested as changes in amount of ablated mass, particle size distribution, etc. The most effective strategy to minimize matrix effects

is the use matrix-match standards. However, fulfilling this requirement is challenging with plant analysis due to significant differences between these samples. Among these differences from unprocessed samples are; water, lignin and cellulose content, and porosity of the surface. In processed samples, for example samples that have undergone drying and grinding, the particle size distribution is an important contributor to natural matrix effects that may lead to poor accuracy and precision in the analysis. Some of these effects could be compensated by lyophilization or cryo-desiccation, optimizing the milling time (to achieve sample homogeneity), the use of a binder (to get better cohesion and flat surfaces of the pellets), and the use of an internal standard (element contained in the sample or by addition to the samples).[17-25]

Internal standard normalization is a powerful alternative successfully used to compensate for matrix effects, and/or improve accuracy and precision in laser ablation-based methods. In the case of optical emission spectrometry (ICP-OES), this approach involves selection of one or more emission lines from an element that is not initially present but added to the sample or a major steady component in the sample (matrix element).[30,31] The selection of a suitable emission line to improve precision relies on the requirement that the behavior of the line(s) will not be affected by slight changes in the matrix, and that the line(s) used for internal standardization is/are simultaneously measured with the lines from the analyte.[32]

In the case of carbon rich samples, selection of carbon as an internal standard seems obvious. This element has been successfully used to compensate for matrix effects and improve accuracy in samples such as rice, milk and coal using LIBS, ICP-OES, and ICP-MS, respectively.[21,33,34] However, in some cases the use of carbon was not satisfactory, for example, no signal correlation was found between analytes of interest and carbon in the study by Todolí et al.[35] These findings were attributed to the generation of two phases during ablation, carbon-

containing gaseous species (CCGS) and a carbon-containing particle (CCP) phase generated during the pyrolysis of the sample. The generation of CCGs and CCP is complex and depends on the composition of the matrix.[36] Finally, normalization with carbon showed improvement for only a few elements in the determination of micronutrients in plants samples using LIBS; this behavior was attributed to differences in ionization and excitation between the elements of interest and carbon.[22]

Another reason for the use of LA-ICP-OES instead of LA-ICP-MS in this particular case is related to the formation of carbon deposits. An incomplete combustion of carbon in the plasma may cause soot deposits thus affecting the plasma stability, and clogging of the sampling cone, which in the case of ICP-MS these problems are more severe than for ICP-OES.

In this study, the efficacy of normalization with carbon (C 193.027nm) added to the sample as a binder in order to improve precision and to compensate matrix effects was evaluated for LA-ICP-OES analysis of plant materials. One approach to expand the concentration range is by diluting these pure samples with a binder, as was described previously, therefore adding binder helps to generate robust pellets, dilute the elemental concentration, and adds the internal standard (in this case carbon).

After the pellets were prepared the first step was to test if the carbon response could be used to improve short-term precision. Second step was to determine if carbon could compensate for changes in the plant matrix due to the addition of binder (synthetic matrix effect). Finally, we tested the possibility of increasing calibration curves dynamic range of concentration by increasing the number of standards within a calibration curve after combining (into one calibration curve) the different plant standard samples.

Results and Discussion

Table 3 presents some figures of merits. Fourteen elements were investigated, and the limits of detection for most of these elements are close to 1 $mg.kg^{-1}$ with the exception of the non-metals S and P. Signal intensity fluctuations (measured as %TRSD) varied in the range 3-44%. However, the reproducibility measured as the difference between three replicates (locations) in the samples was in the range from 3-8 %, even for elements like B, S and Zn that display the highest % TRSD. The reported RSD's in this study are similar to previously reported values using LA-ICP-OES and LIBS[19, 22, 25] In the case of LOD's, it is noticeable that some matrix elements such as Ca, Cu, K, and Mg were significantly better than previously report in the literature.[18,19,21,22,25]

The first step was to test if the carbon response could be used to improve short-term precision. Data in **Figure 1** show the transient ablation response for C, S, Ca and Mg from two tomato leaf samples with 80 % mass fraction of the standard, respectively. **Figure 1 e-g** show the transient ratios of S/C, Ca/C and Mg/C. In every case, the use of carbon as an internal standard slightly improves the short-term precision (%TRSD from 1-5% depending on the element) and is independent of the binder concentration. Similar tendency was obtained with the others mass fractions.

The second step was to determine if carbon could compensate for changes in the plant matrix due to the addition of binder (synthetic matrix effect). **Figure 2a** shows the emission intensity of Ca 317.933 nm as a function of the mass fraction of the apple leaf standards. The emission signal increased with mass fraction of the sample but not linearly, which is an indication of the existence of matrix effects. **Figure 2b** shows the emission intensity for C 193.027 nm from these same pellets. In the case of carbon two clear inflection points in the signal versus mass

fraction of the sample are noticeable. The first inflection point illustrates the change in matrix composition between pure paraffin and paraffin plus 10% plant sample. The second point clearly shows the difference between the combination of paraffin with plant materials and pure plant samples. **Figure 2c** shows the Ca 317.933 nm signal intensity normalized to the C 193.027 nm signal intensity. The intensity ratio exhibits linearity in the analytical range of 10% to 80% of plant content in the pellets. This range contains samples where the physical characteristics of the pellet were similar, such as pellet cohesion and mechanical strength, making the ablation events more reproducible. As shown in **Figure 2c**, carbon normalization can compensate for the synthetic matrix effect created by the addition of binder and can be used as internal standard to improve the calibration curves to sample maximum concentration of 80%. The same behavior was observed for the other NIST plant samples used in this study.

The third step was to increase the number of standards within a calibration curve and to increase the dynamic range of elemental concentration by combining the different plant SRM's. However, only the samples with mass fraction in the range from 10% to 80% were used; the range where the paraffin controls the matrix. Two calibration models were studied. The first calibration model was built with the purpose of studying matrix effects within a set of samples prepared with different mass fractions of a single NIST standard. The second calibration model was obtained combining all NIST standards considered in this study (hybrid approach). In this case, the samples were selected to cover the wider possible range of concentrations.

Figure 3 shows the calibration curves obtained with the NIST spinach samples for P, Mg. Mn, B, Ca, S, Cu and Zn normalized to C. The normalized intensity for all these elements shows linear correlation with the sample mass fractions. Similar results were obtained for the peach, apple and tomato leaf samples (not presented here for brevity).

The final step was to test the combination of these different matrices into one calibration curve per element (hybrid approach). **Figure 4a-c** shows the calibration curves obtained using a combination of the different matrices without normalization, and in **Figure** 4d-f after normalization using the carbon line as an internal standard. These results demonstrate that reduction of matrix effects was achieved within each set of samples (based on the same standard reference material) by using carbon as an internal standard, and between different materials by effectively making the matrix the binder.

A selection of a smaller set of these samples (calibration set) was made and used to build the hybrid calibration curve approach. The criteria used for the selection of the calibration set were: a) samples representing all the matrices, and b) covering the widest concentration range possible. These calibration curves are presented in **Figure 5**. Some of the samples not selected where used as validation samples. The quality of the hybrid calibration models was assessed by calculating the elemental concentration from the validation samples (**Table 4**). Good agreement between the calculated values and known values (% bias) was observed. These results were similar for most elements with a few exceptions of B and Zn in the peach standards. These elements are present in low concentrations in contrast to matrix elements such as Ca, Mg and P that exhibited better accuracy of less than 5% bias (combined). Moreover, it was found that in general, lower % bias was observed in samples with higher elemental concentration such as spinach and tomato samples.

CONCLUSION

Direct solid sampling by Laser Ablation into an Inductively Coupled Plasma Synchronous Vertical Dual View Optical Emission Spectroscope (LA-SVDV-ICP-OES) was, for the first time,

used as for the determination of elemental concentration in plant materials with limit of detection in the single digit mg kg^{-1} levels for most elements. The use of a SVDV-ICP-OES system allows analysis of UV spectral region elements such as P and S axially, with limits of detection as low as 25 mg k^{-1} for S, and elements emitting in the visible region radially, with limits of detection as low as 0.1 mg kg^{-1}.

Carbon was added to the sample as a binder, and was used as an internal standard. The carbon signal was used to normalize the signal of the elements of interest and calibration curves with excellent linear correlations coefficients (better than 0.99 in every case). The use of carbon as internal standard allows for the correction of two types of matrix effects: "natural matrix effect" which is related to the natural differences between the samples, and a "synthetic matrix effect" which is caused by the addition of paraffin to the samples. The impact of the matrix effect correction approach presented in this study allows for the combination of different standard reference materials into a hybrid calibration curve. This was demonstrated by combining samples from each set into a (hybrid) calibration curve, and these new curves were subsequently used to predict the concentration of the samples left out of the model. The results show excellent correlation (low bias percentage) between the calculated concentrations and the known concentration from the validation samples. This strategy can be used to expand the standard materials that can be used in one calibration curve and increase the concentration dynamic range in the quantification models. Although some sample preparation is involved, namely grinding of the samples to equal or less than 75um (size tested in this study), binder addition and mixing with the pure samples followed by pellet pressing, this approach for direct solid analysis is less time-consuming and more efficient than wet sample digestion methods.

ACKNOWLEDGMENTS

The research was supported by the U.S Department of Energy, Office of Basic Energy Sciences, Chemical Science Division at Lawrence Berkeley National Laboratory under contract number DE-AC02-05CH11231.

REFERENCES

01. S. Husted, D. P. Persson, K. H. Laursen, T. H. Hansen, P. Pedas, M. Schiller, J. N. Hegelund, J. K. Schjoerring. "The Role of Atomic Spectrometry in Plant Science". J. Anal. At. Spectrom. 2011, 26(1): 52–79.

02. R. Munson. "Principles of Plant Analysis". In: Y. O. Kalra, editor. Handbook of Reference Methods for Plant Analysis. Boca Raton, Fl, USA: CRC Press, 1998, Chap 1, 1-10.

03. T. H Hansen, K. H Laursen, D. P. Persson, P.i Pedas, S. Husted, J. K. Schjoerring. "Micro-Scaled High-Throughput Digestion of Plant Tissue Samples for Multi-Elemental Analysis". Plant Methods. 2009. 5(12): 1-11.

04. V. Gundersen, I. E. Bechmann, A. Behrens, S. Stürup. "Comparative Investigation of Concentrations of Major and Trace Elements in Organic and Conventional Danish Agricultural Crops. 1. Onions (Allium cepa Hysam) and Peas (Pisum sativum Ping Pong)". J. Agric. Food Chem. 2000. 48(12): 6094–6102.

05. S. R. Oliveira, J. A. G. Neto, J. A. Nobrega, B. T. Jones. "Determination of Macro- and Micronutrients in Plant Leaves by High-Resolution Continuum Source Flame Atomic Absorption Spectrometry Combining Instrumental and Sample Preparation Strategies". Spectrochim. Acta. Part B. 2010. 65(4): 316–320.

06. M. B. Haysom, A. O. Zofia. " Rapid, Wet Oxidative Procedure for the Estimation of Silicon in Plant Tissue". Commun.Soil Sci. Plant Anal. 2006. 37(5): 2299–2306.

07. X. Feng, S. Wu, A. Wharmby, A. Wittmeier. "Microwave Digestion of Plant and Grain Standard Reference Materials in Nitric and Hydrofluoric Acids for Multi-Elemental Determination by Inductively Coupled Plasma Mass Spectrometry". J. Anal. At. Spectrom. 1999. 14(6): 939–946.

08. L. Huang, R. W. Bell, B. Dell, J. Woodward. "Rapid Nitric Acid Digestion of Plant Material with an Open-Vessel Microwave System". Commun. Soil Sci. Plant Anal. 2004. 35(3): 427–440.

09. J. A. V. A. Barros, P. F. de Souza, D. Schiavo, J. A. Nóbrega. "Microwave-Assisted Digestion Using Diluted Acid and Base Solutions for Plant Analysis by ICP OES". J. Anal. At. Spectrom. 2016. 31(1): 337-343.

10. S. L. Costa, M. Miró, E. G. Paranhos, G. D. Matos, P. Sanches, G. Cardoso, W. N. Lopes, A. Tavares, M. G. Rodrigues, R. G. Oliveira. "Slurry Sampling - An Analytical Strategy for the Determination of Metals and Metalloids by Spectroanalytical Techniques". Appl. Spectrosc. 2010. 45:44–62.

11. B Hu, S. Li, G. Xiang, M. He, Z. Jiang. "Recent Progress in Electrothermal Vaporization–Inductively Coupled Plasma Atomic Emission Spectrometry and Inductively Coupled Plasma Mass Spectrometry". Appl. Spectrosc. 2007. 42:203–234.

12. R. E. Russo, X. L. Mao, H. Liu, J. Gonzalez, S. S. Mao. "Laser Ablation in Analytical Chemistry-a Review". Talanta. 2002. **57**(3): 425–451.

13. R. E. Russo, X. Mao, J. Gonzalez, V. Zorba, J. Yoo. "Laser Ablation in Analytical Chemistry". Anal. Chem. 2013. 24(13):6162-6177.

14. R. E. Russo, X. L. Mao, C. Liu, J. Gonzalez. "Laser Assisted Plasma Spectrochemistry: Laser Ablation". J. Anal. At. Spectrom. 2004. 19(9): 1084–1089.

15. J. Koch, D. Gunther. "Review of the State-of-theArt of Laser Ablation Inductively Coupled Plasma Mass Spectrometry". Appl. Spectrosc. 2011. 65(5): 155A-162A.

16. D. W. Hahn, N. Omenetto. "Laser-Induced Breakdown Spectroscopy (LIBS), Part II: Review of Instrumental and Methodological Approaches to Material Analysis and Applications to Different Fields". Appl. Spectrosc. 2012. 66(4): 347-419

17. D. F. Andrade, E. Rodrigues, P. Konieczynski. "Comparison of ICP-OES and LIBS Analysis of Medicinal Herbs Rich in Flavonoids from Eastern Europe". J. Braz. Chem. Soc. 2016. 00:1-10.

18. G. Arantes de Carvalho, J. Moros, D. Santos, F. J. Krug, J. J. Laserna. "Direct Determination of the Nutrient Profile in Plant Materials by Femtosecond Laser-Induced Breakdown Spectroscopy". Anal. Chim. Acta. 2015. 876:26-38.

19. M. Da Silva Gomes, G. G.Arantes de Carvalho, D. Santos, F.J. Krug. "A Novel Strategy for Preparing Calibration Standards for the Analysis of Plant Materials by Laser-Induced Breakdown Spectroscopy: A Case Study with Pellets of Sugar Cane Leaves". Spectrochim. Acta B. 2013. 86: 137–141

20. F. de Souza, D. Santos, G.G.A. de Carvalho, L.C. Nunes, M. Da Silva Gomes, M.B.B. Guerra, F.J Krug. "Determination of Silicon in Plant Materials by Laser-Induced Breakdown Spectroscopy". Spectrochim. Acta B. 2013. 83: 61–65.

21. G. Kim, J. Kwak, J. Choi, K. Park. “Detection of Nutrient Elements and Contamination by Pesticides in Spinach and Rice Samples Using Laser-Induced Breakdown Spectroscopy (LIBS)”. J. Agric. Food Chem. 2012. 60(3): 718–724.

22. J.W.B. Braga, L. C. Trevizan, L. C. Nunes, I. A. Rufini, D. Santos, F.J. Krug. “Comparison of Univariate and Multivariate Calibration for the Determination of Micronutrients in Pellets of Plant Materials by Laser Induced Breakdown Spectrometry”. Spectrochim. Acta B. 2010. 65(4): 66–74.

23. B. Wu, J. S. Becker. “Imaging Techniques for Elements and Element Species in Plant Science”. Metallomics. 2012. 4(5): 403–416.

24. Matheus A.G. Nunes, Monica Voss, Gabriela Corazza, Erico M. M. Flores, Valderi L. Dressler. “External Calibration Strategy for Trace Element Quantification in Botanical Samples by LA-ICP-MS Using Filter Paper. Anal. Chim. Acta. 2016. 905: 51-57

25. M. S. Gomes, E. R. Schenk, D. Santos , F. J. Krug, J. R. Almirall. “Laser Ablation Inductively Coupled Plasma Optical Emission Spectrometry for Analysis of Pellets of Plant Materials”. Spectrochim. Acta B. 2014. 94: 27–33.

26. L. A. Currie, Nomenclature in Evaluation of Analytical Methods Including Detection and Quantification Capabilities (IUPAC recomendations 1995), Pure Appl. Chem 67 (1995) 1699-1723.

27. F. Claverie, B. Fernández, C. Pecheyran, J. Alexis, O. F. X. Donard. “Elemental Fractionation Effects in High Repetition Rate IR Femtosecond Laser Ablation ICP-MS Analysis of Glasses”. J. Anal. At. Spectrom. 2009. 24(7):891–902.

28. J. Fietzke, M. Frische. “ Experimental Evaluation of Elemental Behavior During LA-ICP-MS: Influences of Plasma Conditions and Limits of Plasma Robustness”. J. Anal. At. Spectrom., 2016. 31(1): 234-244.

29. S. Zhang, M. He, Z. Yin, E.i Zhu, W. Hang B. Huang. “Elemental Fractionation and Matrix Effects in Laser Sampling Based Spectrometry”. J. Anal. At. Spectrom. 2016. 31(2): 358-382.

30. N. B. Zorov, A. A. Gorbtenko, T. A Labutin, A. M. Popov. “Review of Normalization Techniques in Analytical Atomic Spectrometry with Laser Sampling: From Single to Multivariate Correction”. Spectrochim. Acta B. 2010, 642-657.

31. M. Grotti, E. Magi, R. Leardi. “Selection of Internal Standards in Inductively Coupled Plasma Atomic Emission Spectrometry by Principal Component Analysis”. J. Anal. At. Spectrom. 2003. 18(3): 274–281

32. C. Dubuisson, E. Poussel, J. M. Mermet. “Comparison of Ionic Line-Based Internal Standardization with Axially and Radially Viewed Inductively Coupled Plasma Atomic Emission

Spectrometry to Compensate for Sodium Effects on Accuracy. J. Anal. At. Spectrom. 1998. 13(11): 1265-1269

33. N. Gilon, J El-Haddad, A. Stankova, W. Lei, Q Ma, V. Motto-Ros, J. Yu. "A Matrix Effect and Accuracy Evaluation for the Determination of Elements in Milk Powder LIBS and Laser Ablation/ICP-OES Spectrometry". Anal. Bioanal Chem. 2011. 401(9): 2681–2689.

34. M. Dong, D. Oropeza, J. Chirinos, J. J. González, J. Lu, X. Mao, R. E. Russo. "Elemental Analysis of Coal by Tandem LIBS and LA-ICP-TOF-MS". Spectrochim. Acta B. 2015. 109:44-50.

35. J. L. Todoli, J. M. Mermet. " Study of Polymer Ablation Products Obtained by Ultraviolet Laser Ablation-Inductively Coupled Plasma Atomic Emission Spectrometry". Spectrochim. Acta B. 1998. 53(12):1645–1656.

36. D. A. Frick, D. Gunther. "Fundamental Studies on the Ablation Behaviour of Carbon in LA-ICP-MS with Respect to the Suitability as Internal Standard". J. Anal. At. Spectrom. 2012. 27(8):1294–1303.

Figure Captions:

Figure 1: (a-d) Transient response for C, S, Ca and Mg from the tomato leaf sample with 80% mass fraction of the standard. (e-g) Transient ratios S/C, Ca/C and Mg/C.

Figure 2: Emission intensity of a) Ca 317.933 nm, b) C 193.027nm and c) Ca/C ratio as a function of the mass fraction of the apple leaf standards.

Figure 3: Calibration curves from the NIST spinach samples for P, Mg. Mn, B, Ca, S, Cu and Zn normalized to C

Figure 4: (a-c) Calibration curves using a combination of the different matrices without normalization, and (d-f) after normalization using the carbon line as internal standard.

Figure 5: Hybrid calibration approach for P, Mg, Mn, B, Ca, S, Cu and Zn normalized to C.

Table Captions:

Table1: Experimental conditions of the LA-ICP-OES system.

Table 2. NIST Standard Reference Materials concentrations.

Table 3. Analytical figure of merits achieved for the apple SRM 1515.

Table 4: Prediction using NIST plant samples at different dilution factors.

Table1: Experimental conditions of the LA-ICP OES

ICP OES Agilent 5100	
Power, W	1200
Plasma Ar gas flow rate, L min^{-1}	8.00
Auxiliary Ar gas flow rate, Lmin^{-1}	0.80
Make-up He gas flow rate, L min^{-1}	0.70
Viewing mode:	SVDV
Read time, s	1
Total acquisition time, s	25
Working wavelengths, nm	B I 249.772, C I 193.027, Ca II 396,847, Ca II 317.993, K I 769.897, Cu II 324.754, Mg II 280.270, Fe II 259.940, Mn II 257.610, Na I 589.592, P I 213.618, S I 181.972, Sr II 407.771, Zn I 213.857
Laser Ablation System J-200 Applied Spectra	
Wavelength, nm	213
Pulse energy, mJ	4
Fluence, J cm^{-2}	17
Repetition rate, Hz	10
Pre-ablation time, s	15
Scan speed, mm s^{-1}	0.025
Carrier He gas flow rate, L min^{-1}	0.70

Table 2. NIST Standard Reference Materials concentrations

SRM	Description	Mg	Ca	Fe	Al	K	Na	Mn	Cr	Ni	Zn	Ba	Pb	Cu	Sr	V	P	Cl	S	Th	U	N
1515	Apple leaves	0.271*	1.526*	(83)	286	1.61*	24.4	54	(0.3)	0.91	12.5	49	0.47	5.64	25	0.26	0.159*	579	(0.18*)	(0.03)	(0.006)	2.25*
1547	Peach leaves	0.432*	1.56*	(218)	249	2.43*	24	98	(1)	0.69	17.9	124	0.87	3.7	53	0.37	0.137*	360	(0.2*)	(0.05)	(0.015)	2.94*
1570a	Spinach leaves	(0.89*)	1.527*		310	2.903*	1.818*	75.9		2.14	82			12.2	55.6	0.57	0.518*		(0.46*)	0.048	0.155	6.06*
1573a	Tomato leaves	(1.2*)	5.05*	368	598	2.70*	136		1.99	1.59	30.9	63		4.7	85	0.835	0.216*	(6600)	(0.96*)	(0.12)	(35)	3.03*

Elemental composition as mass fraction in mg/kg (ppm) unless noted by an * for %.

Table 3. Some analytical figure of merits achieved with Apple SRM 1515

Element	Wavelength, nm	LOD, $mg*Kg^{-1}$	TRSD %	RSD, %
S	181.972	50	31	8
P	213.618	25	19	2
Zn	213.857	0.4	44	4
B	249.772	0.4	30	5
Mn	257.610	0.1	11	3
Fe	259.940	1	14	5
Mg	280.270	0.2	9	1
Cu	324.754	0.2	20	5
Al	396.152	3	13	5
Sr	407.771	0.1	10	5
Ca	317.933	4	12	3
Ba	455.403	3	10	1
Na	589.592	0.8	16	6
K	769.897	22	3	2

Figure 1a-d: show transient response for C, S, Ca and Mg from the tomato leave sample with 80% mass fraction of the standard. And e-g show the transient ratios S/C, Ca/C and Mg/C.

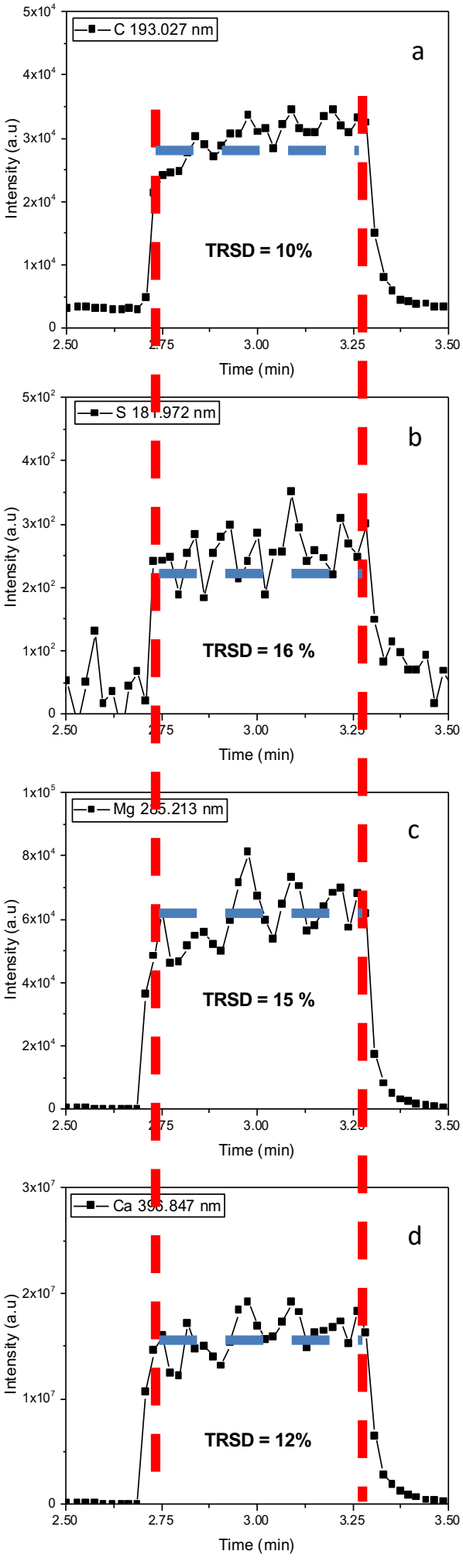

Tomato 80 %

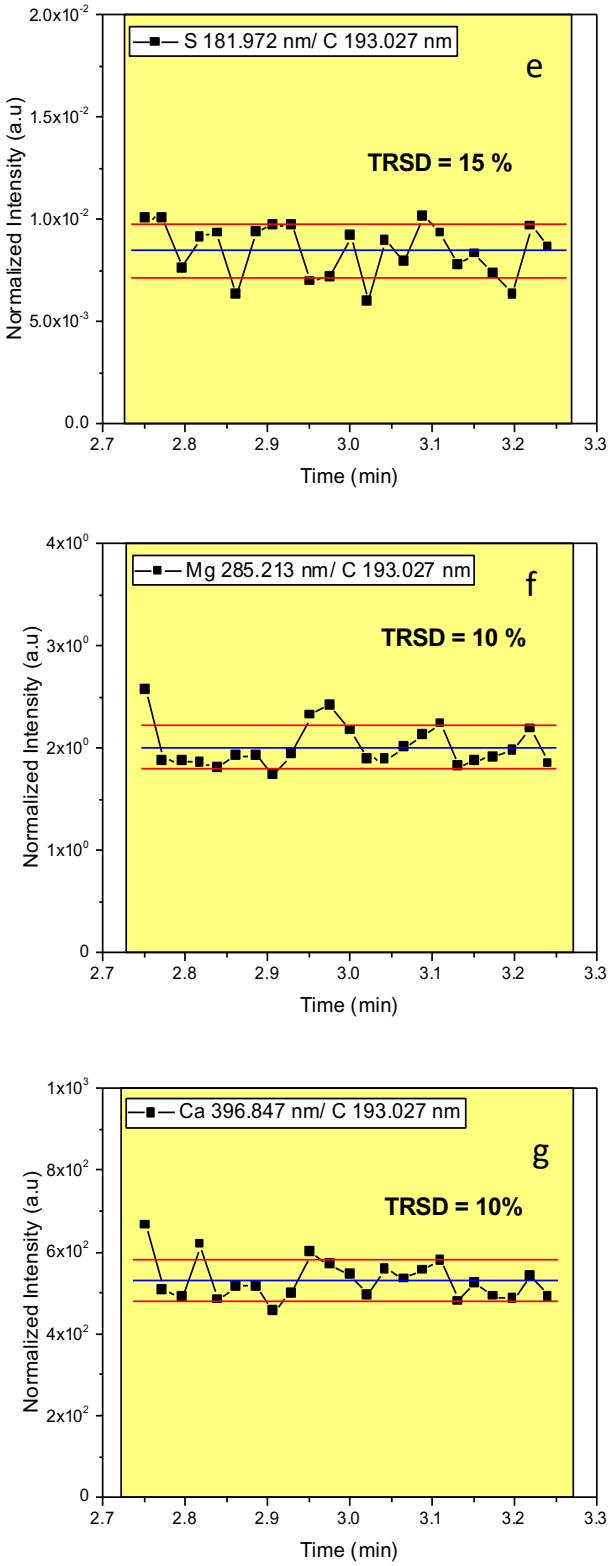

Figure 2: Emission intensity of a) Ca 317.933 nm, b) C 193.027nm and c) Ca/C ratio as function of the mass fraction of the apple leaves standards

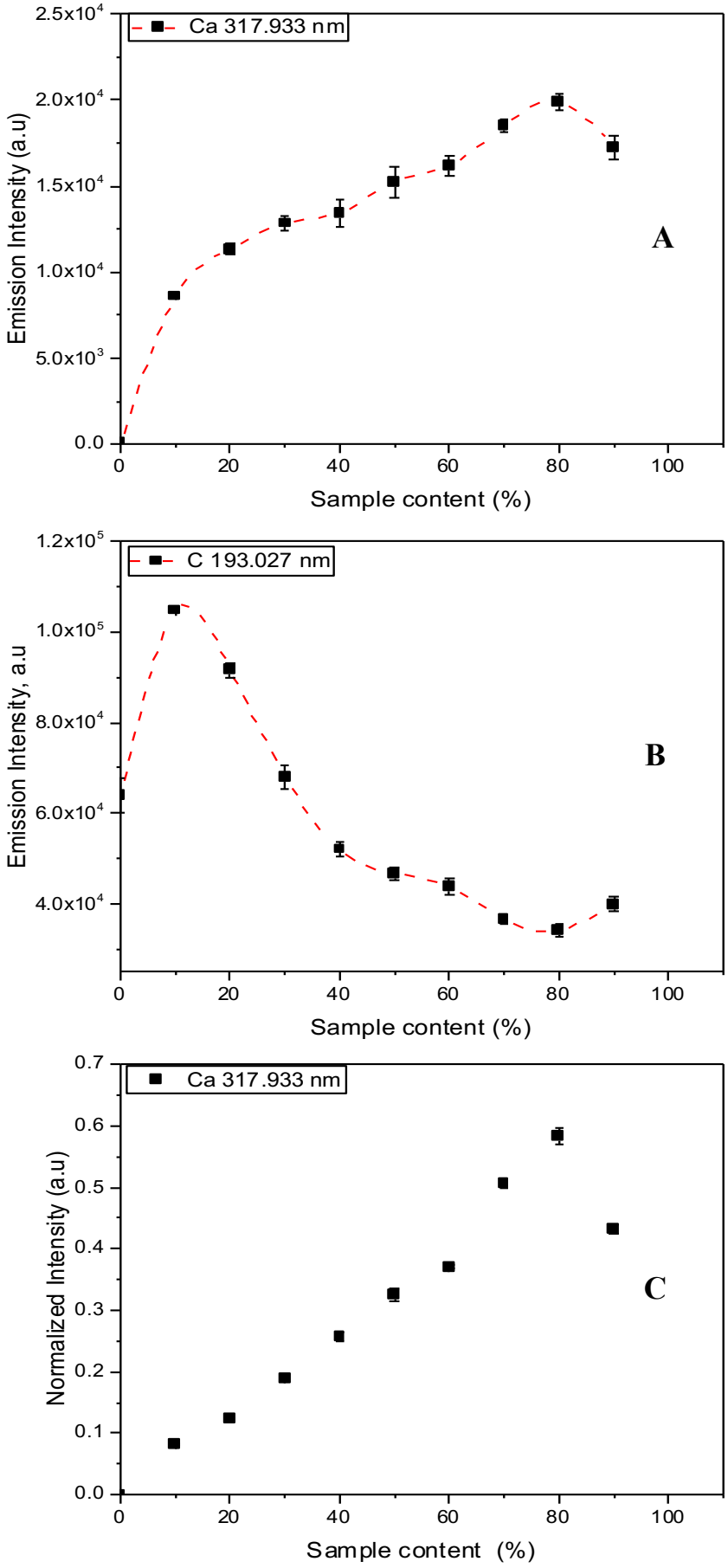

Figure 3: Calibration curves from NIST spinach samples for P, Mg. Mn, B, Ca, S, Cu and Zn normalized to C

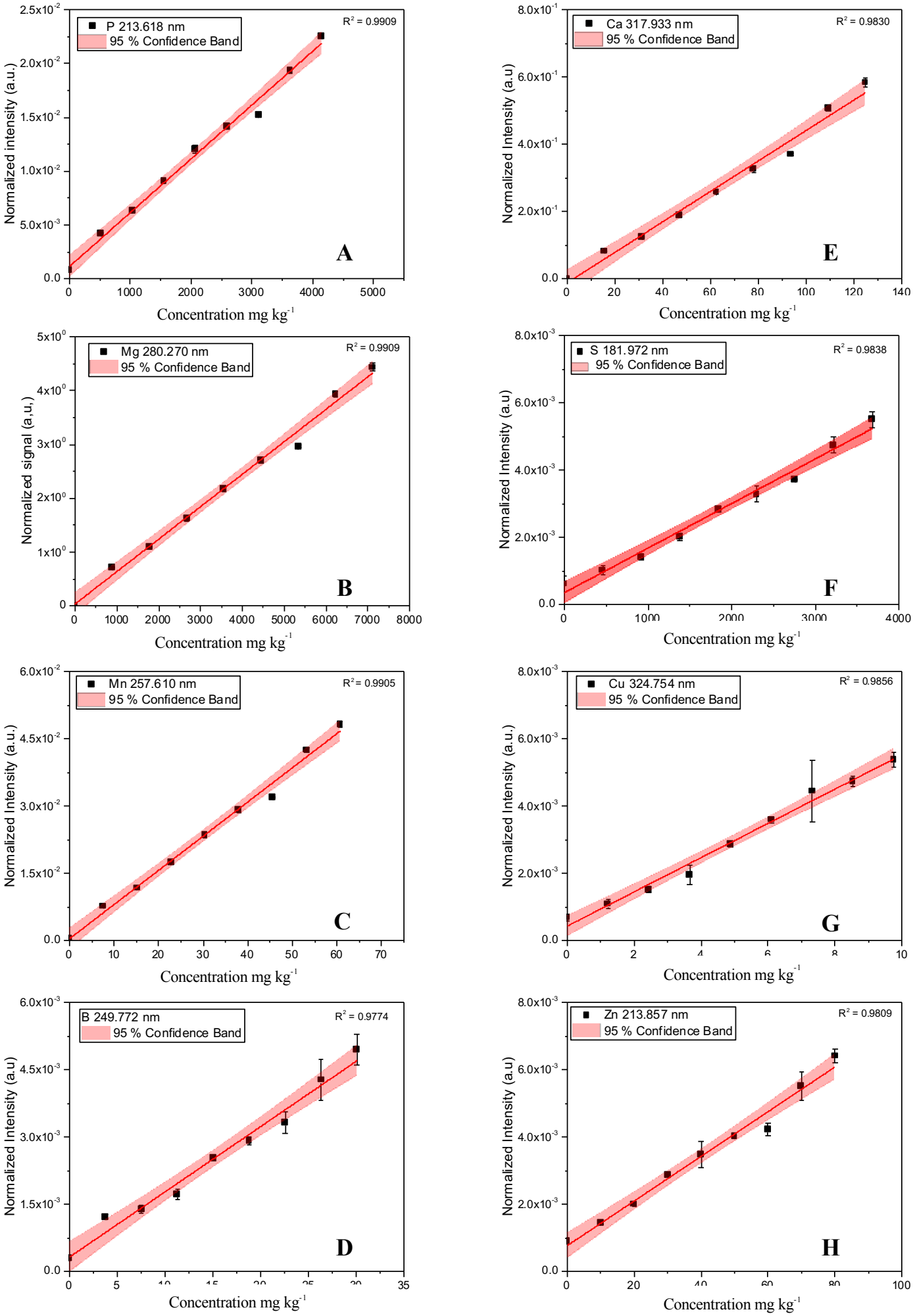

Figure 4: a-c) shows the calibration curves using a combination of the different matrices without normalization, and figure d-f) after normalization using carbon line as internal standard

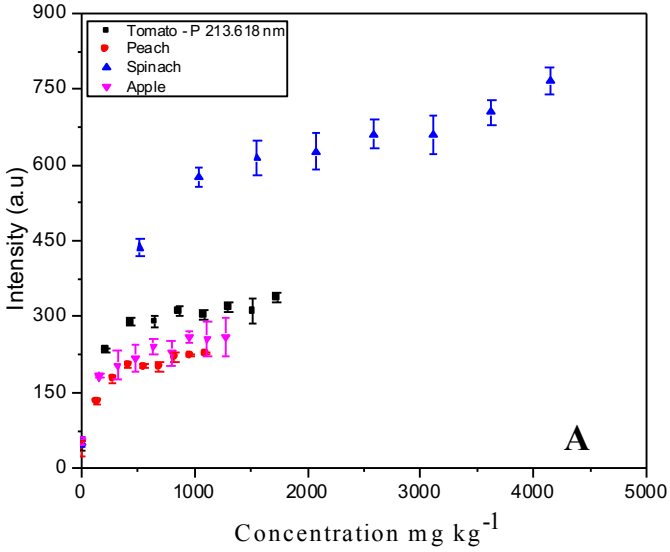

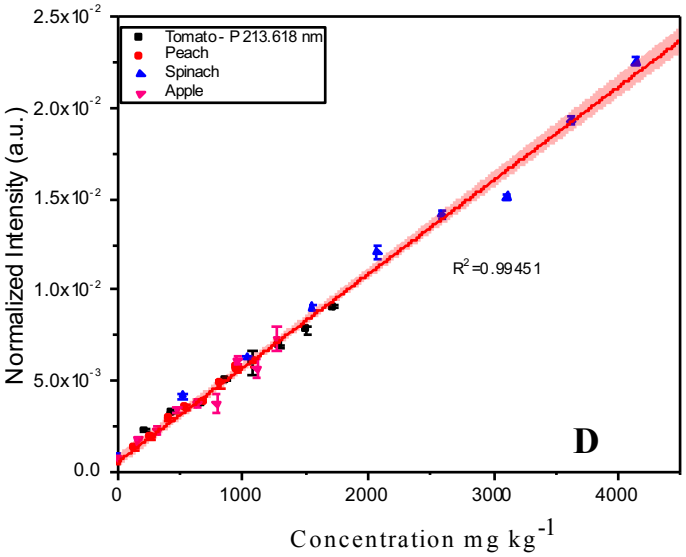

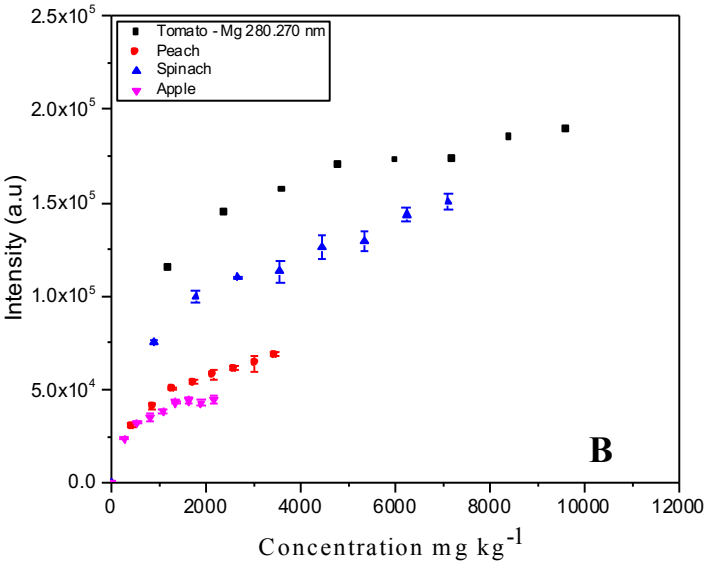

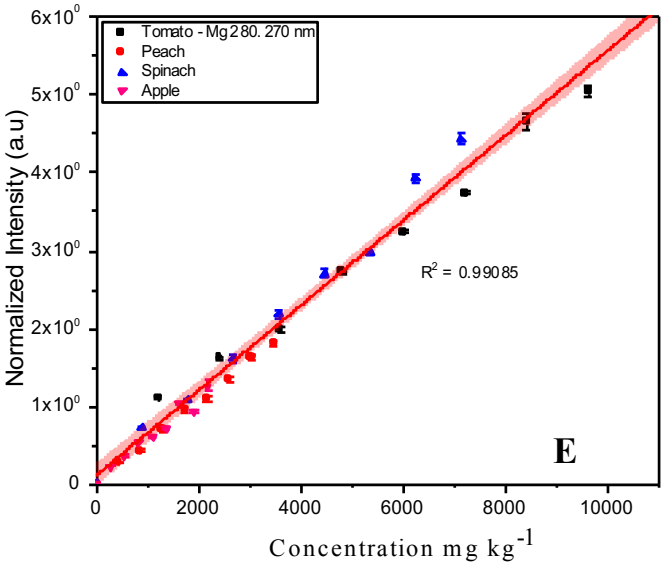

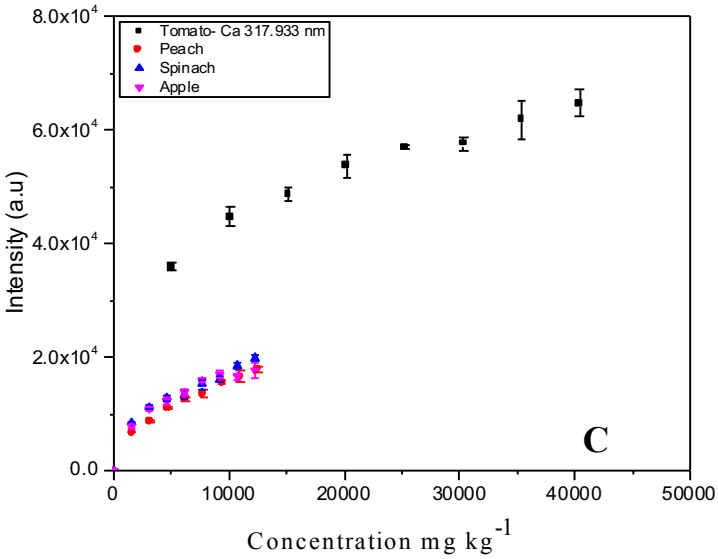

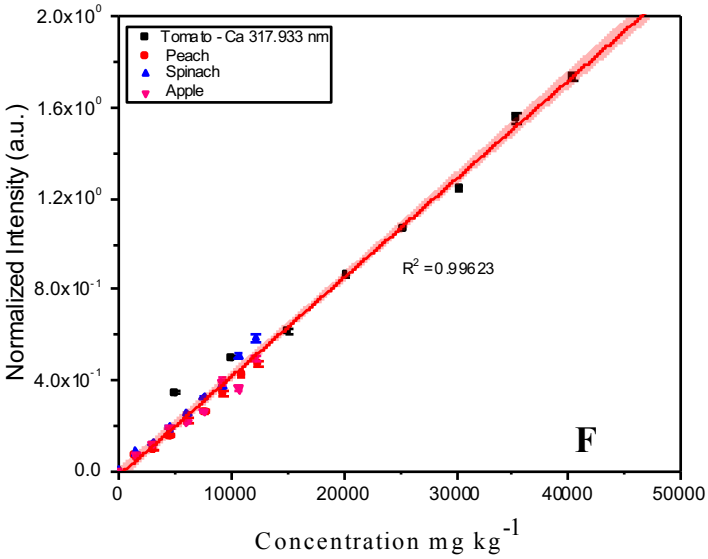

Figure 5: Hybrid calibration approach for P, Mg, Mn, B, Ca, S, Cu and Zn normalized to C

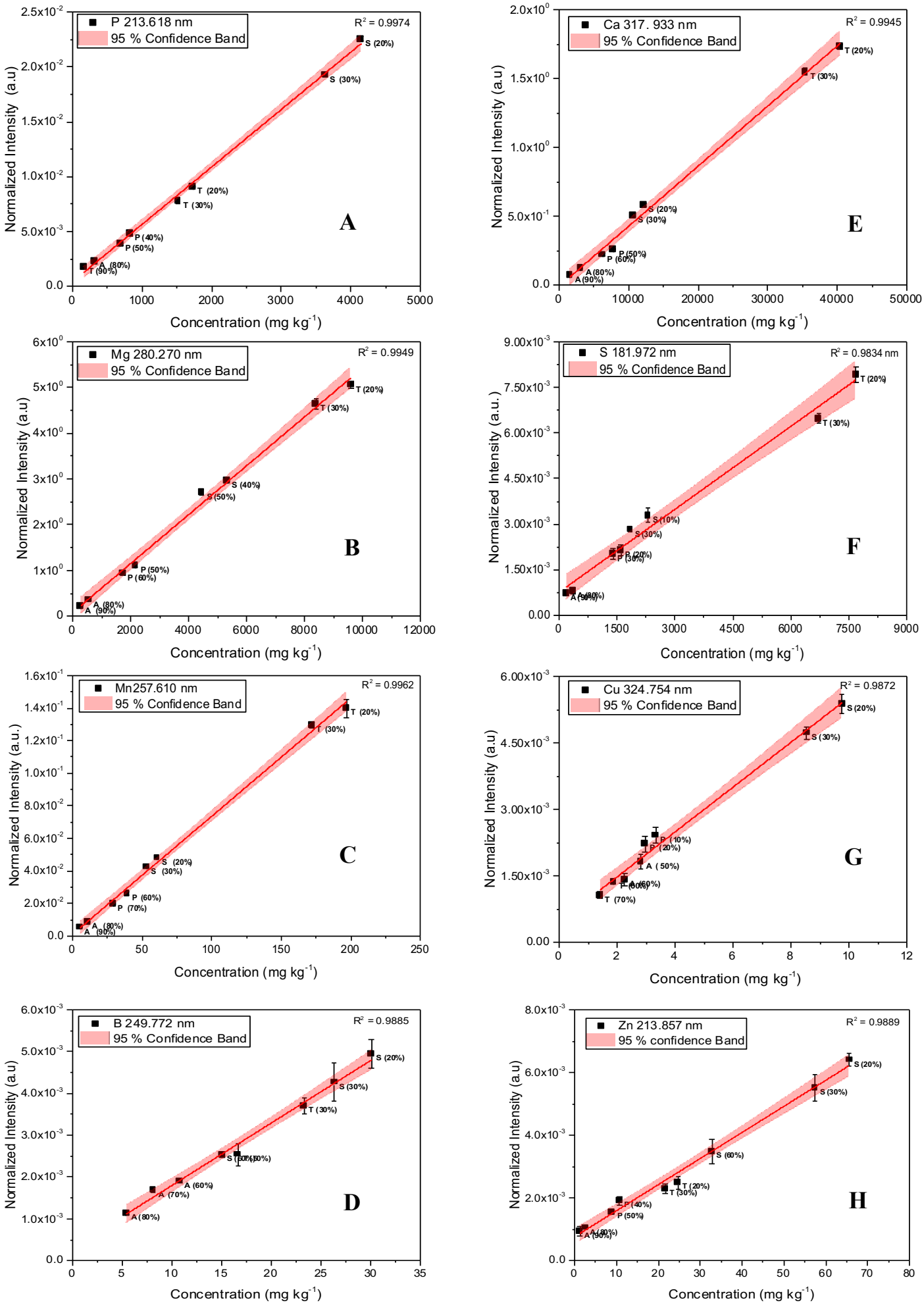

Note: A: Apple, P: Peach, S: Spinach T: Tomato. Values in parenthesis are the binder concentration in the pellet

Table 4: Prediction using NIST Plant Samples having different dilution factors

Element/wavelength	Certified Value ($mg\ Kg^{-1}$)	Dilution factor	Obtained ($mg\ Kg^{-1}$)	Bias (%)	Dilution factor	Obtained ($mg\ Kg^{-1}$)	Bias (%)
Spinach							
B 249.772 nm	37.6	5.00	36 ± 2	-4	3.33	33 ± 2	-14
Ca 317.933 nm	15270	5.00	15094 ± 2970	-1	3.33	15070 ± 2943	-1
Cu 324.754 nm	12.2	5.00	10 ± 1	-16	3.33	9.2 ± 0.9	-25
Mg 280.270 nm	8900	5.00	9412 ± 671	6	3.33	9626 ± 660	9
Mn 257.610 nm	75.9	5.00	74 ± 12	-3	3.33	75 ± 12	-0.7
P 213.618 nm	5180	5.00	5600 ± 221	8	3.33	5499 ± 220	6
S 181.972 nm	4600	5.00	3617 ± 986	- 18	3.33	4595 ± 971	- 0.1
Zn 213.857 nm	82	5.00	75 ± 9	-9	3.33	84 ± 9	2
Tomato							
B 249.772 nm	33.3	2.5	30 ± 1	- 9	2.00	30 ± 1	- 9
Ca 317.933 nm	50500	2.5	49807 ± 2883	-1	2.00	51795± 2962	2.6
Cu 324.754 nm	4.7	2.5	4.4 ± 0.9	-6	2.00	5.5 ± 0.9	17
Mg 280.270 nm	12000	2.5	12390 ± 657	3	2.00	12440 ± 670	3.7
Mn 257.610 nm	246	2.5	251 ± 12	2	2.00	251 ± 12	2.0
P 213.618 nm	2160	2.5	2189 ± 223	1	2.00	2135 ± 222	-1.2
S 181.972 nm	9600	2.5	8595 ± 960	-10	2.00	8663 ± 975	-9.8
Zn 213.857 nm	30.9	2.5	20 ± 9	-35	2.00	26 ± 9	-16
Peach							
B 249.772 nm	29	1.67	23 ± 1	- 20	1.43	75 ± 1	159
Ca 317.933 nm	15600	1.67	13364 ± 2895	- 14.3	1.43	14053 ± 2879	-9.9
Cu 324.754 nm	3.7	1.67	4.3 ± 0.9	16. 2	1.43	5.1 ± 0.9	38
Mg 280.270 nm	4320	1.67	3935 ± 665	-9	1.43	4120 ± 659	-5
Mn 257.610 nm	98	1.67	83 ± 12	-15	1.43	87± 12	-11
P 213.618 nm	1370	1.67	1405 ± 224	2.6	1.43	1438 ± 222	5
S 181.972 nm	2000	1.67	1923 ± 976	-3.9	1.43	1985 ± 970	-0.8
Zn 213.857 nm	17.9	1.67	23 ± 9	17.3	1.43	27± 9	45
Apple							
B 249.772 nm	27	1.43	18 ± 2	-17	1.25	32 ± 2	4
Ca 317.933 nm	15260	1.43	12229 ± 2890	-20	1.25	14524 ± 2867	-4.8
Cu 324.754 nm	5.64	1.43	4.2 ± 0.9	- 26	1.25	7.7± 0.9	37
Mg 280.270 nm	2710	1.43	2304 ± 675	-15	1.25	2768 ± 666	2
Mn 257.610 nm	54	1.43	41± 12	-24	1.25	51 ± 12	-6
P 213.618 nm	1590	1.43	1427 ± 222	-10	1.25	1640 ± 220	3
S 181.972 nm	1800	1.43	1288 ± 979	-39	1.25	2035 ± 970	2.3
Zn 213.857 nm	12.5	1.43	20 ± 9	3.2	1.25	26 ± 9	-108